AIP | Applied Physics Letters

One-dimensional photonic crystal nanobeam lasers on a flexible substrate

Tsan-Wen Lu, Li-Hsun Chiu, Pin-Tso Lin, and Po-Tsung Lee

Citation: Appl. Phys. Lett. **99**, 071101 (2011); doi: 10.1063/1.3626592
View online: http://dx.doi.org/10.1063/1.3626592
View Table of Contents: http://apl.aip.org/resource/1/APPLAB/v99/i7
Published by the AIP Publishing LLC.

One-dimensional photonic crystal nanobeam lasers on a flexible substrate

Tsan-Wen Lu, Li-Hsun Chiu, Pin-Tso Lin, and Po-Tsung Lee[a)]
Department of Photonics & Institute of Electro-Optical Engineering, National Chiao Tung University, Rm. 415 CPT Building, 1001 Ta-Hsueh Road, Hsinchu 30010, Taiwan.

(Received 11 May 2011; accepted 29 July 2011; published online 15 August 2011)

We demonstrate a one-dimensional (*1D*) photonic crystal (PhC) nanocavity laser composed of hybrid *PhC* mirrors on a suspended nanobeam (NB) with very small device footprint of 8.5×0.57 μm^2. The *0th*-order mode lasing action with low threshold of 280 μW is observed. Via the optical glue stamping process, the devices are directly transferred onto a flexible polypropylene substrate. Single mode lasing action with effective threshold of 17 μW is achieved. The robust lasing properties of the device with different bending radii R from ∞ to 2.5 mm are obtained. Via finite-element method, we also theoretically address that the lasing wavelength is almost invariant when $R > 1.0$ mm. This flexible *1D PhC* NB laser will be a good candidate for efficient nanolaser in future flexible photonic integrated circuits with ultrahigh component density. © *2011 American Institute of Physics*. [doi:10.1063/1.3626592]

Recently, various flexible micro- and nano-photonic devices have been proposed and demonstrated, including one-(*1D*),[1] two- (*2D*),[2] three-dimensional (*3D*)[3,4] photonic crystals (PhCs), micro-disk,[5] and so on, which are used for tunable optical filter,[1,2] strain,[3,4] and curvature[5] sensors. This kind of flexible device not only can be utilized in micro electro mechanical systems, but also could play a pioneering role in realizing the flexible photonic integrated circuits (fPICs). However, up to date, an efficient and robust nanolaser,[6] which has long been regarded as an essential for constructing *PICs*, has not been demonstrated on a flexible platform yet. Very recently, *1D PhC* nanocavities on nanobeams (NBs)[7,8] with high quality (Q) factors and small mode volumes have drawn lots of attentions. Owing to the simple architecture, easy fusion with waveguide system,[9] and much smaller footprint than 2D PhC devices, *1D PhC* NB nanocavity is a good candidate for the robust nanolasers[10–13] in fPICs. In this report, we demonstrate a *1D PhC* single defect nanocavity laser on NB with small device footprint and low threshold. Subsequently, via the optical glue stamping process, the NB lasers (NBLs) are directly transferred onto a flexible polymer substrate. Low lasing threshold and robust lasing properties of the NBLs with different bending radii are obtained. The invariant lasing wavelength and the bending limitation are also confirmed and investigated theoretically by *3D* finite-element method (FEM).

Scheme of *1D PhC* nanocavity on a suspended *InGaAsP* NB is shown in Fig. 1(a). *1D PhCs* are composed of air holes, and the nanocavity is consisted of a central missing air hole, the tapered and outer *PhC* mirrors. The air hole radius (r) over lattice constant (a) (r/a) ratio of the tapered *PhC* mirror is fixed at 0.37 with linearly varied a from 330 to 430 nm, which is designed for efficiently reducing the scattering losses from the cavity to the outer *PhC* mirror.[14] The lattice constant of the cavity region is defined as a_c and the cavity size L defined in Fig. 1(b) is 420 nm. The period numbers of the tapered and outer *PhC* mirrors (N_{tap} and N_{out}) are four and six. The index (n_{NB}), width w, and thickness t of the *InGaAsP* NB are 3.4 nm, 570 nm, and 220 nm. With above parameters, via *3D* FEM, the *0th*-order mode profile in electric-field and its normalized frequency are shown in Fig. 1(a). The simulated Q and mode volume are 8000 and 0.040 μm^3 ($\sim 0.47\ (\lambda/n_{NB})^3$), respectively.

The *1D PhC* NBL is realized on *InGaAsP* multi-quantum-wells (MQWs) epitaxial structure with 220 nm thickness grown on *InP* substrate. 140 nm SiN_x layer is subsequently deposited on the MQWs to serve as a hard mask. Then, the positive electron-beam (e-beam) resist is spun-coated on the SiN_x. The fabrication process is followed by e-beam lithography for defining *PhC* patterns and reactive ion etching/inductively coupled plasma dry etching for the pattern transferring into the SiN_x and MQWs layers. The SiN_x residue is removed by buffered oxide etch. We then use the diluted HCl wet etching at 2 °C to form the suspended NB and smooth the device surface. Top- and tilted-view scanning electron microscope (SEM) pictures of *1D PhC* NBL are shown in Fig. 1(b). The r/a ratio is 0.37 with a varied from 330 (cavity) to 430 nm (outer *PhC* mirror), and the w keeps constant around 570 nm via proximity correction during e-beam lithography.

Then, the devices are mounted on a 3-axis piezo-stage and excited at room temperature by an 845 nm diode laser with 15 ns pulse width and 150 kHz repetition rate. The laser emissions are collected via an optical fiber and analyzed by an optical spectrum analyzer. The light-in light-out (L-L) curve and single mode lasing spectrum from the NBL in Fig. 1(b) are shown in Fig. 1(c). The lasing wavelength at 1498 nm agrees with the simulated frequency ($a_c/\lambda = 0.2207$) of the *0th*-order mode, which shows a very low threshold of 280 μW owing to ultrasmall mode volume of the *0th*-order mode. Considering the effective pumping area (pump spot size $\sim$ 4.2 μm in diameter) and the power absorbed by the MQWs, the effective threshold is as low as 8.5 μW. In addition, once we move the pump spot from the cavity to the tapered *PhC* mirror, no lasing action is observed, which confirms that the lasing mode well localizes within the nanocavity. The measured NBL polarization as the inset of Fig. 1(c) shows a linear polarized ratio of 1:4.3. We should note that the length of *1D PhC* NBL with $N_{out} = 6$ is only 8.5 μm, which leads to a very small device footprint of 8.5×0.57 μm^2.

[a)]Electronic mail: potsung@mail.nctu.edu.tw.

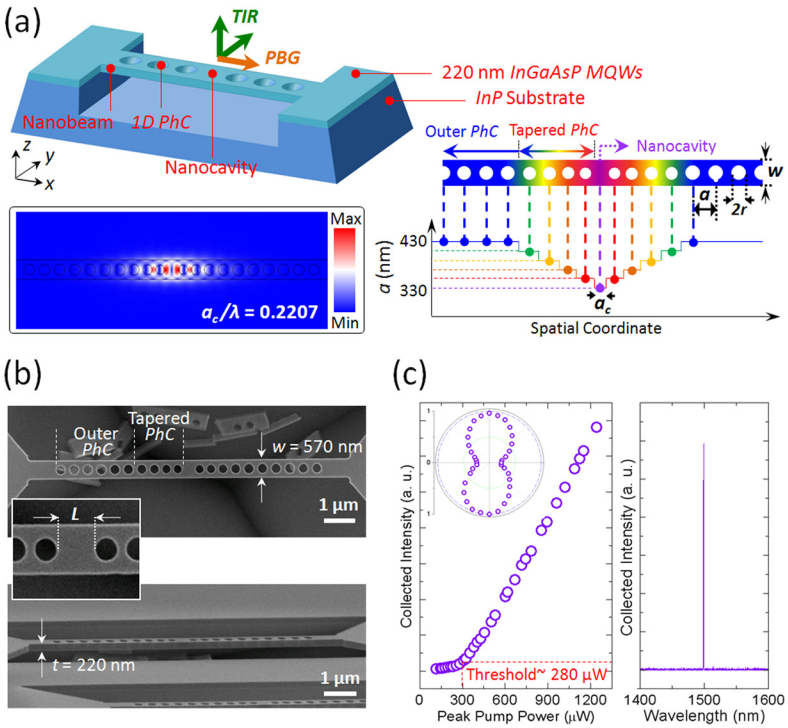

FIG. 1. (Color online) (a) Scheme of *1D PhC* single defect nanocavity with the tapered and outer *PhC* mirrors on a suspended InGaAsP NB. The *0th*-order mode profile in electric-field and its normalized frequency by *3D* FEM are also shown. (b) Top- and tilted-view SEM pictures of *1D PhC* nanocavity with $L = 420$ nm, $t = 220$ nm, $r/a = 0.37$, $w = 570$ nm, and $N_{out} = 6$ on NB. (c) The *L-L* curve (left) and single-mode lasing spectrum (right) of the NBL shown in (b). The measured polarization is also shown as the inset.

We also fabricate the NBLs with different N_{out} from fifteen to three. The *0th*-order mode lasing action is still observed when $N_{out} = 3$, while the device footprint is further reduced to be $6.0 \times 0.57\ \mu m^2$.

To realize the flexible NBLs (fNBLs), we apply an acrylic-based optical glue (refractive index ~ 1.48) stamping process,[1,15,16] as illustrated in Fig. 2(a), which can directly transfer the NBLs onto a flexible polypropylene substrate. In measurements, the *L-L* curve and single mode lasing spectrum of the fNBL are shown in Figs. 2(b) and 2(c), which show a threshold of 630 μW and the lasing wavelength at 1575 nm. The higher threshold of the fNBL than that of suspended NBL is arisen from the increased optical losses due to the decreased index contrast between the NB and the optical glue. However, the effective threshold of 17 μW is still sufficiently low for an efficient nanolaser. The wavelengths under different pump powers are also shown in Fig. 2(b), which helps to confirm the lasing threshold. The carrier density and substrate temperature both increase with the pump power, which contribute negative and positive index variations to the nanocavity, respectively. The increasing carrier density is dominant in wavelength shift owing to the alleviated substrate heating under pulsed pumping. As a result, wavelength blue-shift with increase in the pump power is observed. Above threshold, the increasing rate of carrier density slows down. Thus, the wavelength shows different blue-shift rates below and above threshold.[17] In addition, we also observe that the lasing linewidth increases with the pump power above threshold. The lasing spectra of the NBL before and after being transferred onto the flexible substrate are shown in Fig. 2(c). A significant wavelength red-shift of 46 nm is observed, which is caused by the increased effective index due to the optical glue and agrees well with the simulated wavelength red-shift of 42 nm.

We further investigate the lasing properties of the fNBL with different bending radii R. In experiments, the fNBL with shortened nanocavity size L of 390 nm is employed to retard the cavity deformation when bending. This also leads to an increased Q factor of 3×10^4 and decreased mode volume of 0.033 μm^3. The fNBL is fixed on the home-made mounts with different R, as shown in Fig. 3(a). The single-mode lasing spectra, lasing wavelengths, and linewidths of

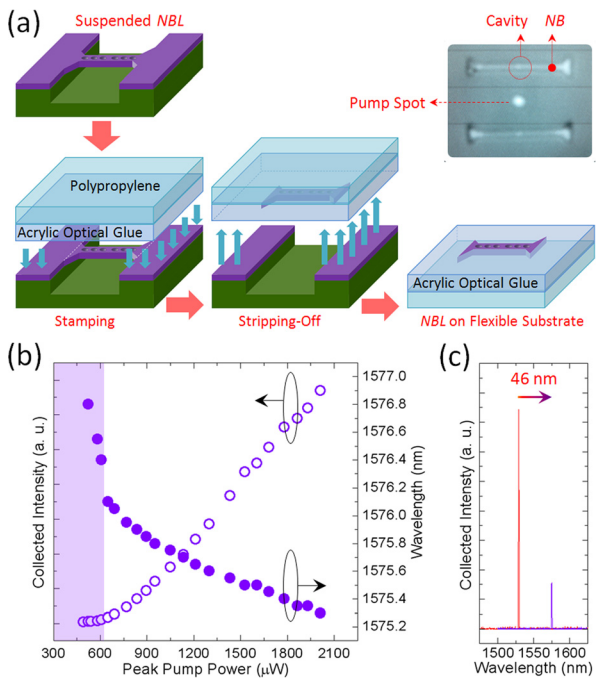

FIG. 2. (Color online) (a) Illustration of transferring the NBLs onto a flexible substrate. The inset image shows how the pump spot and the NB nanocavity look like separately under the optical microscope. (b) The *L-L* curve and the lasing wavelengths under different pump powers. The designed nanocavity size L of the characterized NBL is 440 nm. (c) The lasing spectra of the NBL before (shorter wavelength) and after (longer wavelength) being transferred onto the flexible substrate.

the fNBL under different R and strictly fixed pump power of 1 mW are shown in Figs. 3(b) and 3(c). We find that the laser emission intensity (4.8% variation), lasing wavelength (0.15 nm variation), and linewidth (0.1 nm variation), are almost invariant under different R from ∞ (without bending) to 2.5 mm. The available minimum bending radius in experiments is limited by the mount we can make. These results show the robust lasing properties of the fNBL because the bending radius range in experiments only leads to very slight deformation of the nanocavity with relatively small cavity size.

To confirm above assumption and investigate the bending limitation of the fNBL theoretically, we employ *3D* FEM simulation with triangular and non-uniform meshes, which provides sufficient flexibility to precisely resolve the bending of *1D PhC* NBL. In simulations, the radius elongations and rotations of air holes due to the NB bending are considered and illustrated in Fig. 3(d), which are 0.36% elongation in x-direction and $0.3/a_c$ when $R = 0.0625$ mm. The simulated wavelengths of the *0th*-order mode under different R from 5 to 0.0625 mm are shown in Fig. 3(e). The wavelength is almost invariant when $R > 1.0$ mm, which confirms our measurement results. Once the R becomes smaller than 1.0 mm, the wavelength shows a significant red-shift, which is caused by the considerable nanocavity elongation due to the NB bending. The simulated mode profiles in electric-fields of the *0th*-order mode when $R = \infty$ (without bending) and 0.0625 mm are shown as the insets of Fig. 3(e).

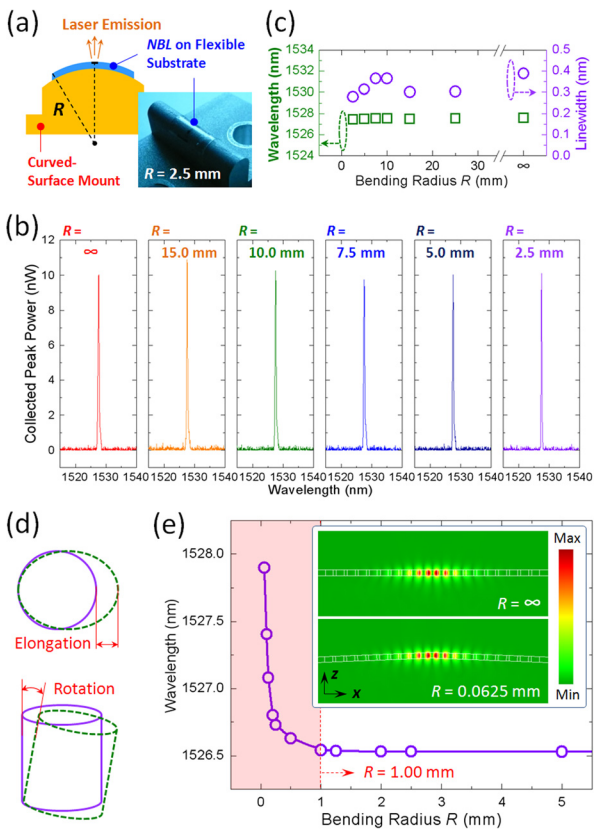

FIG. 3. (Color online) (a) Scheme and picture of the fNBL on the home-made mount surface with bending radius R. The (b) lasing spectra, (c) lasing wavelengths, and linewidths of the fNBL with reduced cavity size L of 390 nm under different R from ∞ to 2.5 mm. (d) Scheme of the radius elongation and rotation of the air hole due to the NB bending in simulations. (e) The FEM simulated wavelength of the fNB nanocavity under different R from 5.0 to 0.0625 mm. The wavelength shows a significant red-shift when $R < 1.0$ mm. The simulated mode profiles in electric-fields of the fNB nanocavity when $R = \infty$ and 0.0625 mm are shown as the insets.

In summary, we demonstrate a *1D PhC* single defect nanocavity composed of hybrid tapered/outer *PhC* mirrors on a suspended *InGaAsP* NB. In experiments, the *0th*-order mode lasing with ultralow threshold of 280 μW (effective threshold of 8.5 μW) is obtained from the NBL with six outer *PhC* mirror periods, which corresponds to a very small device footprint of $8.5 \times 0.57\ \mu m^2$. Via the optical glue stamping process, the NBLs are directly transferred onto a flexible substrate and single mode lasing with low effective threshold of 17 μW is obtained. Owing to the small device footprint and cavity size of the presented NB nanocavity, the fNBL shows robust lasing properties under bending radii from ∞ to 2.5 mm, including the almost invariant laser emission intensity, lasing wavelength, and linewidth. Via *3D* FEM, we confirm the almost invariant lasing wavelength and find the bending radius limitation of 1.0 mm for the presented fNBL. We believe this *1D PhC* fNBL with low threshold, small device footprint, and robust lasing properties with different bending radii will be very suitable for serving as an efficient nanolaser in future fPICs with ultrahigh component density.

This work is supported by Taiwan's National Science Council (NSC) under Contract Numbers NSC-98-2221-E-009-015-MY2 and NSC-100-2120-M-009-005. The authors would like to thank the help from Center for Nano Science and Technology (CNST) of National Chiao Tung University (NCTU), Taiwan.

[1]C. Jansen, S. Wietzke, V. Astley, D. M. Mittleman, and M. Koch, Appl. Phys. Lett. **96**, 111108 (2010).
[2]W. Zhou, Z. Ma, H. Yang, Z. Qiang, G. Qin, H. Pang, L. Chen, W. Yang, S. Chuwongin, and D. Zhao, J. Phys. D: Appl. Phys. **42**, 234007 (2009).
[3]O. L. J. Pursiainen, J. J. Baumberg, H. Winkler, B. Viel, P. Spahn, and T. Ruhl, Adv. Mater. **20**, 1484 (2008).
[4]O. L. J. Pursiainen, J. J. Baumberg, K. Ryan, J. Bauer, H. Winkler, B. Viel, and T. Ruhl, Appl. Phys. Lett. **87**, 101902 (2005).
[5]M. H. Shih, K. S. Hsu, W. Kunag, Y. C. Yang, Y. C. Wang, S. K. Tsai, Y. C. Liu, Z. C. Chang, and M. C. Wu, Opt. Lett. **34**, 2733 (2009).
[6]S. Noda, Science **314**, 260 (2006).
[7]M. Notomi, E. Kuramochi, and H. Taniyama, Opt. Express **16**, 11095 (2008).
[8]P. B. Deotare, M. W. McCutcheon, I. W. Frank, M. Khan, and M. Lončar, Appl. Phys. Lett. **94**, 121106 (2009).
[9]Q. Quan, P. B. Deotare, and M. Lončar, Appl. Phys. Lett. **96**, 203102 (2010).
[10]B. H. Ahn, J. H. Kang, M. K. Kim, J. H. Song, B. Min, K. S. Kim, and Y. H. Lee, Opt. Express **18**, 5654 (2010).
[11]Y. Gong, B. Ellis, G. Shambat, T. Sarmiento, J. S. Harris, and J. Vučković, Opt. Express **18**, 8781 (2010).
[12]Y. Zhang, M. Khan, Y. Huang, J. Ryou, P. Deotare, R. Dupuis, and M. Lončar, Appl. Phys. Lett. **97**, 051104 (2010).
[13]R. Perahia, J. D. Cohen, S. Meenehan, T. P. M. Alegre, and O. Painter, Appl. Phys. Lett. **97**, 191112 (2010).
[14]Y. Akahane, T. Asano, B. S. Song, and S. Noda, Nature **425**, 944 (2003).
[15]M. J. Zablocki, A. Sharkawy, O. Ebil, and D. W. Prather, Opt. Lett. **36**, 58 (2011).
[16]Z. Qiang, H. Yang, L. Chen, H. Pang, Z. Ma, and W. Zhou, Appl. Phys. Lett. **93**, 061106 (2008).
[17]L. Lu, A. Mock, M. Bagheri, J. R. Cao, S. J. Choi, J. O'Brien, and P. D. Dapkus, IEEE Photon. Technol. Lett. **21**, 1166 (2009).